Biomechanics and Modeling in Mechanobiology (2018) 17:1875–1883
https://doi.org/10.1007/s10237-018-1062-3

ORIGINAL PAPER

An elasto-viscoplastic model to describe the ratcheting behavior of articular cartilage

Yilin Zhu[1,2]

Received: 1 March 2018 / Accepted: 24 July 2018 / Published online: 4 August 2018

Abstract
In the present work, a constitutive model for articular cartilage is proposed in finite elasto-viscoplasticity. For simplification, articular cartilage is supposed to be a typical composite composed of a soft basis and a fiber assembly. The stress tensor and free energy function are hence accordingly divided into two components. The high nonlinear stress-strain response is assumed to be mainly related to the fiber assembly and described by an exponential-type hypoelastic relation. Ratcheting is considered according to the viscoplasticity, the evolution rule of which is deduced from the dissipative inequality by the co-directionality hypotheses. Then, the capability of the proposed model is validated by comparing its predictions with related experimental observations. Results show that the ratcheting behavior and stress-strain hysteresis loops are reasonably captured by the proposed model.

Keywords Articular cartilage · Constitutive model · Logarithmic stress rate · Ratcheting

1 Introduction

Articular cartilage, the connective tissue covering the surface of the subchondral bone in diarthrodial joints, plays a crucial role in shock absorption, load transmission and sustainability. As observed by researchers (Gao et al. 2015; Sophia Fox et al. 2009), articular cartilage suffers both dynamic and static loads, which may be up to ten times the bodyweight in daily living. Therefore, the biomechanical property of articular cartilage needs to be understood. This topic has attracted much attention, and many achievements have been made both experimentally and theoretically. As reported by Li et al. (2005), Responte et al. (2007) and Athanasiou et al. (2009), articular cartilage is a typical highly functional multiphase material that has some special features, i.e., high nonlinearity and viscocity. Based on the experimental observations, many constitutive models have been presented to simulate the biomechanical behaviors of articular cartilage (Armstrong et al. 1984; Ateshian 2017; Bursać et al. 1999; García and Cortés 2006; Huang et al. 2001; Kwan et al. 1990; Mow et al. 1980; Pierce et al. 2013; Seifzadeh et al. 2012; Soltz and Ateshian 2000a; Wilson et al. 2005). However, the existing research is mainly focused on describing the biomechanical responses under monotonic loading conditions, e.g., the monotonic stress-strain relationship and the creep and stress relaxation behavior.

It should be noted that articular cartilage suffers complicated cyclic loads in daily living (Barker and Seedhom 2001; Soltz and Ateshian 2000b). Since the mechanical fatigue caused by cyclic loading is assumed to be one of the major causes of osteoarthritis (Kurz et al. 2005), the cyclic deformation behavior of articular cartilage has also attracted attention. Barker and Seedhom (2001) experimentally studied the cyclic compressive deformation of articular cartilage from human cadaveric knee joints. Bellucci and Seedhom (2001) performed cyclic tensile tests of articular cartilage from the human knee to investigate the topographic and zonal variations in the fatigue behavior. Kerin et al. (2003) investigated the surface fissure propagation of articular cartilage of cow by cyclic loading tests in vitro. Gao et al. (2013) studied the depth-dependent strain fields of porcine articular cartilage under cyclic rolling load by an optimized digital image correlation technique.

However, the ratcheting behavior of articular cartilage was not investigated in the above-mentioned studies. Ratchet-

✉ Yilin Zhu
lin5210feng@163.com

[1] School of Architectural and Civil Engineering, Chengdu University, Chengdu 610106, People's Republic of China

[2] School of Electromechanical Automobile Engineering, Yantai University, Yantai 264005, People's Republic of China

ing is the inelastic strain accumulation under asymmetrical force/stress-controlled cyclic loading conditions, which may play an important role in assessing the wear property as well as fatigue life of the materials (Gao et al. 2015; Kang 2008; Kang and Wu 2011; Zhu et al. 2014a, b). The ratcheting behavior of metals (Kang 2008), polymeric materials (Chen and Hui 2005; Lu et al. 2016), composite materials (Ahmadzadeh and Varvanifarahani 2015; Guo et al. 2013) and biologic tissues (Kang and Wu 2011; Zhu et al. 2014b) was thus studied systematically. When the cartilage is subjected to cyclic loading, fatigue damage may occur in the cartilage joint because of accumulation of ratcheting strain (Gao et al. 2015). It is thus also important to investigate the ratcheting behavior of articular cartilage. Recently, Gao et al. (2015) carried out detailed experimental observations of the ratcheting behavior of articular cartilage under stress-controlled cyclic compressive loading conditions. In the experimental tests, the used material was the fresh articular cartilage of the knee joint from an 8-month-old pig. The dimensions of the experimental samples were approximately 5.5 mm long, 4.5 mm wide and 12 mm thick. To maintain the physiologic environment of cartilage, all samples were soaked in saline before the tests. An Electronic Universal Fatigue Testing System (EUF-1020) was used for all the tests. The experimental results showed that the ratcheting behavior of porcine articular cartilage depends strongly on the loading level and rate. Given that the ratcheting behavior of articular cartilage has not been considered by the previous constitutive models (Armstrong et al. 1984; Ateshian 2017; Bursać et al. 1999; García and Cortés 2006; Huang et al. 2001; Kwan et al. 1990; Mow et al. 1980; Pierce et al. 2013; Seifzadeh et al. 2012; Soltz and Ateshian 2000a; Wilson et al. 2005), a constitutive model for articular cartilage considering ratcheting is proposed in the present work. The current model is constructed in the framework of finite elasto-viscoplasticity theory by incorporating the logarithmic stress rate. According to experimental observations (Athanasiou et al. 2009; Li et al. 2005; Matzat et al. 2013; Responte et al. 2007), articular cartilage is a typical multiphase material composed of electrolytes, fluid, collagen fibers, proteoglycans, chondrocytes, etc. (as shown in Fig. 1). The fiber network mainly contributes strength and stiffness to the material. Therefore, in this work, articular cartilage is simply supposed to be composed of a fiber assembly (related to the collagen fibers) and a soft basis (related to the other components). Both parts contribute to the free energy and stress functions. The nonlinearity is considered as an exponential-type nonlinear elastic relation for the fiber assembly. Ratcheting is reflected by the viscoplasticity, the evolution rule of which is formulated from the Clausius-Duhem inequality by co-directionality hypotheses. The prediction ability of the presented model is finally validated by comparing the predictions with related experimental observations (Gao et al. 2015). It is shown that the ratcheting behavior as well as the cyclic stress-strain responses of articular cartilage is reasonably captured by the proposed model.

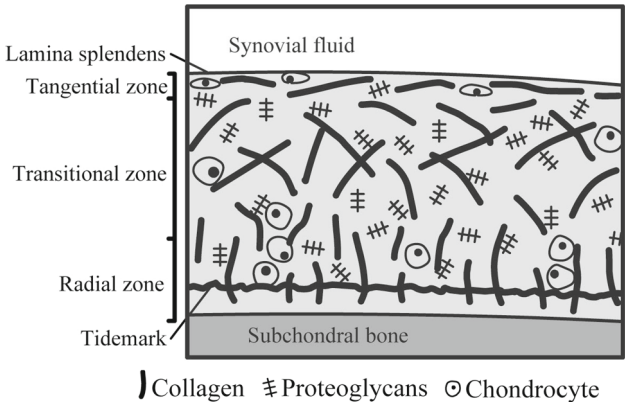

Fig. 1 Microstructure of articular cartilage

2 Proposed model

Based on the thermodynamic laws and logarithmic stress rate, an elasto-viscoplastic model to describe the ratcheting behavior of articular cartilage is presented in this section, which consists of three parts and is structured as follows:

In Sect. 2.1, some information on the kinematics and logarithmic stress rate are introduced; in Sect. 2.2, the free energy function is presented and the dissipative inequality derived; in Sect. 2.3, the stress functions and inelastic evolution equations are proposed.

2.1 Kinematics and logarithmic rate

In the present work, a constitutive model is developed in a rate type based on a finite elasto-plastic theory, the kinematics of which are as follows:

$$\mathbf{F} = \frac{\partial \mathbf{x}}{\partial \mathbf{X}}, \quad \mathbf{L} = \frac{\partial \dot{\mathbf{x}}}{\partial \mathbf{X}} = \dot{\mathbf{F}}\mathbf{F}^{-1}, \tag{1}$$

$$\mathbf{F} = \mathbf{V}\mathbf{R}, \quad \mathbf{R}^{\mathrm{T}} = \mathbf{R}^{-1}, \quad \mathbf{B} = \mathbf{V}^2, \tag{2}$$

$$\mathbf{D} = \mathrm{sym}\mathbf{L}, \quad \mathbf{W} = \mathrm{skw}\mathbf{L}, \tag{3}$$

$$\mathbf{h} = \ln \mathbf{V}, \tag{4}$$

where $\mathbf{F}$ and $\mathbf{L}$ are respectively the deformation gradient tensor and velocity tensor; $\mathbf{x}$ and $\mathbf{X}$ are respectively the spatial and related material vectors; $\mathbf{R}$ is an orthogonal rotation tensor; $\mathbf{V}$ and $\mathbf{B}$ are respectively the left stretch and left Cauchy-Green tensors; $\mathbf{D}$ (the symmetric part of $\mathbf{L}$) and $\mathbf{W}$ (the skew part of $\mathbf{L}$) are the stretching tensor and spin tensor, respectively; $\mathbf{h}$ is Hencky's strain.

As reported by Bruhns et al. (1999) and Xiao et al. (1997a, b), only if the logarithmic stress rate is introduced are the constitutive models in rate type developed by hypo-elasticity self-consistent with the notion of elasticity. Besides, the logarithmic rate of Hencky's strain $\mathbf{h}$ and the stretching tensor $\mathbf{D}$ are equal to each other, i.e.,

$$\overset{\circ}{\mathbf{h}}{}^{\log} = \left(\ln \overset{\circ}{\mathbf{V}}\right)^{\log} = \mathbf{D}, \tag{5}$$

with $\overset{\circ}{\mathbf{A}}{}^{\log}$, the logarithmic rate of an arbitrary symmetric second-order tensor $\mathbf{A}$, defined as

$$\overset{\circ}{\mathbf{A}}{}^{\log} = \dot{\mathbf{A}} + \mathbf{A}^{\log} - \boldsymbol{\Omega}^{\log}\mathbf{A}, \tag{6}$$

where $\boldsymbol{\Omega}^{\log}$ is the skew logarithmic spin, which is a function of the left stretch tensor $\mathbf{B}$ and the stretching tensor $\mathbf{D}$. More details can be found in Bruhns et al. (1999) and Xiao et al. (1997a, b).

Furthermore, there is a time-dependent rotation $\mathbf{R}^{\log}$, which can be used to define the logarithmic spin $\boldsymbol{\Omega}^{\log}$ as follows:

$$\dot{\mathbf{R}}^{\log} = \boldsymbol{\Omega}^{\log}\mathbf{R}^{\log}, \tag{7}$$

with the initial condition $\left(\mathbf{R}^{\log}\right)_{t=0} = \mathbf{1}$.

According to Bruhns et al. (1999), we have

$$\mathbf{A} : \overset{\circ}{\mathbf{A}}{}^{\log} = \mathbf{A} : \dot{\mathbf{A}}. \tag{8}$$

$$\frac{\mathrm{d}}{\mathrm{d}t}\left(\mathbf{Q}^{\mathrm{T}}\mathbf{A}\mathbf{Q}\right) = \mathbf{Q}^{\mathrm{T}}\overset{\circ}{\mathbf{A}}{}^{\log}\mathbf{Q}. \tag{9}$$

where $\mathbf{Q}$ is an orthogonal tensor.

2.2 Free energy function and thermodynamic restrictions

As mentioned in Sect. 1, the articular cartilage is simply considered a typical composite material consisting of a fiber assembly and a soft basis.

Hence, the Kirchhoff stress tensor $\boldsymbol{\tau}$ can be decomposed into two contributions, i.e.,

$$\boldsymbol{\tau} = \boldsymbol{\tau}^{\mathrm{b}} + \boldsymbol{\tau}^{\mathrm{f}}, \tag{10}$$

where $\boldsymbol{\tau}^{\mathrm{b}}$ and $\boldsymbol{\tau}^{\mathrm{f}}$ are respectively the stress components associated with the basis and fiber assembly.

Suppose that the basis and fiber assembly have an identical deformation, indicating that

$$\mathbf{h} = \mathbf{h}^{\mathrm{b}} = \mathbf{h}^{\mathrm{f}}. \tag{11}$$

For elasto-viscoplastic theory, Hencky's strain $\mathbf{h}$ is further additively decomposed as:

$$\mathbf{h}^{\mathrm{b}} = \mathbf{h}^{\mathrm{e(b)}} + \mathbf{h}^{\mathrm{vp(b)}}, \quad \mathbf{h}^{\mathrm{f}} = \mathbf{h}^{\mathrm{e(f)}} + \mathbf{h}^{\mathrm{vp(f)}}, \tag{12}$$

where $\mathbf{h}^{\mathrm{e(b)}}$ and $\mathbf{h}^{\mathrm{e(f)}}$ are respectively the elastic strain tensors related to the basis and fiber assembly, and $\mathbf{h}^{\mathrm{vp(b)}}$ and $\mathbf{h}^{\mathrm{vp(f)}}$ represent the viscoplastic strain tensors related to the basis and fiber assembly, respectively.

According to Zhu et al. (2014a, 2016), in large deformation, Eqs. (11) and (12) can be directly replaced by

$$\mathbf{D} = \mathbf{D}^{\mathrm{b}} = \mathbf{D}^{\mathrm{f}}, \tag{13}$$

$$\mathbf{D}^{\mathrm{b}} = \mathbf{D}^{\mathrm{e(b)}} + \mathbf{D}^{\mathrm{vp(b)}}, \quad \mathbf{D}^{\mathrm{f}} = \mathbf{D}^{\mathrm{e(f)}} + \mathbf{D}^{\mathrm{vp(f)}}, \tag{14}$$

where $\mathbf{D}^{\mathrm{e(b)}}$, $\mathbf{D}^{\mathrm{e(f)}}$ and $\mathbf{D}^{\mathrm{vp(b)}}$ and $\mathbf{D}^{\mathrm{vp(f)}}$ represent the elastic stretching tensors and viscoplastic stretching tensors related to the basis and fiber assembly, respectively. In addition, it supposes

$$\mathbf{D}^{\mathrm{e(b)}} = \overset{\circ}{\mathbf{h}}{}^{\log(\mathrm{e(b)})}, \quad \mathbf{D}^{\mathrm{e(f)}} = \overset{\circ}{\mathbf{h}}{}^{\log(\mathrm{vp(f)})}. \tag{15}$$

Assuming plastic Hencky strains, $\mathbf{h}^{\mathrm{vp(b)}}$ and $\mathbf{h}^{\mathrm{vp(f)}}$ are strictly dissipated; the free energy ψ is hence supposed to be a function of the elastic Hencky strains $\mathbf{h}^{\mathrm{e(b)}}$ and $\mathbf{h}^{\mathrm{e(f)}}$, i.e.,

$$\psi = \hat{\psi}\left(\mathbf{h}^{\mathrm{e(b)}}, \mathbf{h}^{\mathrm{e(f)}}\right). \tag{16}$$

Neglecting the coupling effect, ψ can be additively decomposed as

$$\psi = \hat{\psi}^{\mathrm{b}}\left(\mathbf{h}^{\mathrm{e(b)}}\right) + \hat{\psi}^{\mathrm{f}}\left(\mathbf{h}^{\mathrm{e(f)}}\right), \tag{17}$$

where $\hat{\psi}^{\mathrm{b}}$ and $\hat{\psi}^{\mathrm{f}}$ represent the free energy function components associated with the contributions of the basis and fiber assembly, respectively.

Restricting to isothermal conditions, the dissipative inequality is given as

$$\boldsymbol{\tau} : \mathbf{D} - \dot{\psi} \geq 0. \tag{18}$$

In view of Eq. (17), the time derivative of the free energy ψ is obtained as

$$\dot{\psi} = \frac{\partial \hat{\psi}^{\mathrm{b}}}{\partial \mathbf{h}^{\mathrm{e(b)}}} : \dot{\mathbf{h}}^{\mathrm{e(b)}} + \frac{\partial \hat{\psi}^{\mathrm{f}}}{\partial \mathbf{h}^{\mathrm{e(f)}}} : \dot{\mathbf{h}}^{\mathrm{e(f)}}. \tag{19}$$

According to Zhu et al. (2016), for initially isotropic elasticity, if ψ is a quadratic function of $\mathbf{h}^{\mathrm{e(b)}}$ and $\mathbf{h}^{\mathrm{e(f)}}$, Eq. (17) can be rewritten with Eqs. (7) and (12–15) as

$$\dot{\psi} = \frac{\partial \hat{\psi}^{\mathrm{b}}}{\partial \mathbf{h}^{\mathrm{e(b)}}} : \left(\mathbf{D} - \mathbf{D}^{\mathrm{vp(b)}}\right) + \frac{\partial \hat{\psi}^{\mathrm{f}}}{\partial \mathbf{h}^{\mathrm{e(f)}}} : \left(\mathbf{D} - \mathbf{D}^{\mathrm{vp(f)}}\right). \quad (20)$$

Hence, Eq. (18) is reformulated as

$$\left(\boldsymbol{\tau} - \frac{\partial \hat{\psi}^{\mathrm{b}}}{\partial \mathbf{h}^{\mathrm{e(b)}}} - \frac{\partial \hat{\psi}^{\mathrm{f}}}{\partial \mathbf{h}^{\mathrm{e(f)}}}\right) :\mathbf{D} + \frac{\partial \hat{\psi}^{\mathrm{b}}}{\partial \mathbf{h}^{\mathrm{e(b)}}} :\mathbf{D}^{\mathrm{vp(b)}} + \frac{\partial \hat{\psi}^{\mathrm{f}}}{\partial \mathbf{h}^{\mathrm{e(f)}}} :\mathbf{D}^{\mathrm{vp(f)}} \geq 0. \quad (21)$$

It is reduced as

$$\boldsymbol{\tau}^{\mathrm{b}} : \mathbf{D}^{\mathrm{vp(b)}} + \boldsymbol{\tau}^{\mathrm{f}} : \mathbf{D}^{\mathrm{vp(f)}} \geq 0. \quad (22)$$

with the following definitions

$$\boldsymbol{\tau}^{\mathrm{b}} = \frac{\partial \hat{\psi}^{\mathrm{b}}}{\partial \mathbf{h}^{\mathrm{e(b)}}}, \ \boldsymbol{\tau}^{\mathrm{f}} = \frac{\partial \hat{\psi}^{\mathrm{f}}}{\partial \mathbf{h}^{\mathrm{e(f)}}} \quad (23)$$

2.3 Constitutive equations

Commonly, a linear hypoelastic relationship can be assumed by adopting Hooker's law. However, a highly nonlinear stress-strain response (generally J-shaped) of articular cartilage is observed according to the experimental research (Gao et al. 2015).

Such a nonlinearity is mainly caused by the fibers having different lengths and only undertaking loads after certain critical stress/strain. Therefore, a nonlinear elastic relationship for $\boldsymbol{\tau}^{\mathrm{f}}$ is introduced in this work. The elastic relations related to $\boldsymbol{\tau}^{\mathrm{b}}$ and $\boldsymbol{\tau}^{\mathrm{f}}$ are respectively formulated as

$$\overset{\circ}{\boldsymbol{\tau}}{}^{\mathrm{log(b)}} = 2\mu^{\mathrm{b}}\overset{\circ}{\mathbf{h}}{}^{\mathrm{log(e(b))}} + \lambda^{\mathrm{b}}\mathrm{tr}\left(\overset{\circ}{\mathbf{h}}{}^{\mathrm{log(e(b))}}\right)\mathbf{1} = \mathbb{C}^{\mathrm{b}} : \mathbf{D}^{\mathrm{e(b)}}, \quad (24a)$$

and

$$\overset{\circ}{\boldsymbol{\tau}}{}^{\mathrm{log(f)}} = 2\mu^{\mathrm{f}}\overset{\circ}{\mathbf{h}}{}^{\mathrm{log(e(f))}} + \lambda^{\mathrm{f}}\mathrm{tr}\left(\overset{\circ}{\mathbf{h}}{}^{\mathrm{log(e(f))}}\right)\mathbf{1} = \mathbb{C}^{\mathrm{f}} : \mathbf{D}^{\mathrm{e(f)}}, \quad (24b)$$

where $\mathbb{C}^{\mathrm{b}}$ and $\mathbb{C}^{\mathrm{f}}$ are the fourth-order elastic tensors; $\mu^i = \frac{E^i}{2(1+\nu^i)}$ $(i = \mathrm{b},\ \mathrm{f})$ and $\lambda^i = \frac{\nu^i E^i}{(1+\nu^i)(1-2\nu^i)}$ $(i = \mathrm{b}, \mathrm{f})$ are the Lamé constants ($E^{\mathrm{b},\,\mathrm{f}}$ are the Young's modulus and $\nu^{\mathrm{b},\,\mathrm{f}}$ are the Poisson ratios); $\mathbf{1}$ is the second-order identity tensor. To describe the nonlinearity, E^{f} is supposed to be evolved as

$$E^{\mathrm{f}} = \beta\left(\alpha + \bar{\tau}^{\mathrm{f}}\right), \quad (25)$$

Table 1 Summary of the proposed model

Strain	$\mathbf{h} = \mathbf{h}^{\mathrm{b}} = \mathbf{h}^{\mathrm{f}}$
Deformation partition	$\mathbf{L} = \frac{\partial \dot{\mathbf{R}}}{\partial \mathbf{X}} = \dot{\mathbf{F}}\mathbf{F}^{-1} = \mathbf{D}+\mathbf{W}$; $\mathbf{D} = \frac{1}{2}(\mathbf{L} + \mathbf{L}^{\mathrm{T}})$, $\mathbf{W} = \frac{1}{2}(\mathbf{L} - \mathbf{L}^{\mathrm{T}})$; $\mathbf{D} = \mathbf{D}^{\mathrm{b}} = \mathbf{D}^{\mathrm{f}}$, $\mathbf{D}^{\mathrm{b}} = \mathbf{D}^{\mathrm{e(b)}} = \mathbf{D}^{\mathrm{vp(b)}}$, $\mathbf{D}^{\mathrm{f}} = \mathbf{D}^{\mathrm{e(f)}} = \mathbf{D}^{\mathrm{vp(f)}}$
Hypo-elastic relation	$\overset{\circ}{\boldsymbol{\tau}}{}^{\mathrm{log}} = \overset{\circ}{\boldsymbol{\tau}}{}^{\mathrm{log(b)}} + \overset{\circ}{\boldsymbol{\tau}}{}^{\mathrm{log(f)}}$, $\overset{\circ}{\boldsymbol{\tau}}{}^{\mathrm{log(b)}} = \mathbb{C}^{\mathrm{b}} : \mathbf{D}^{\mathrm{e(b)}}$, $\overset{\circ}{\boldsymbol{\tau}}{}^{\mathrm{log(f)}} = \mathbb{C}^{\mathrm{f}} : \mathbf{D}^{\mathrm{e(f)}}$, $E^{\mathrm{f}} = \beta(\alpha + \bar{\tau}^{(\mathrm{f})})$
Viscoplastic flow rules	$\mathbf{D}^{\mathrm{vp(b)}} = \gamma^{\mathrm{b}}\boldsymbol{\tau}'^{\mathrm{b}}$; $\mathbf{D}^{\mathrm{vp(f)}} = \gamma^{\mathrm{f}}\boldsymbol{\tau}'^{\mathrm{f}}$, $\gamma^{\mathrm{f}} = \gamma_0^{\mathrm{f}} + (\gamma_{\mathrm{sat}}^{\mathrm{f}} - \gamma_0^{\mathrm{f}})(1 - \exp(-\rho p^f))$, $\dot{p}^{\mathrm{f}} = \sqrt{\frac{2}{3}}\|\mathbf{D}^{\mathrm{vp(f)}}\|$

Table 2 Load cases used in ratcheting tests of articular cartilage

Load cases	Stress amplitude (MPa)	Stress rate (MPa)	Cycles (N)
A	0.5		100
	1.0	0.1	
	1.5		
B		0.1	
	1.0	0.2	
		0.4	

Table 3 Material parameters for articular cartilage in the proposed model

$E^{\mathrm{b}} = 2.0$ Mpa, $\nu^{\mathrm{b}} = 0.48$, $\gamma^{\mathrm{b}} = 0.2$; $\nu^{\mathrm{f}} = 0.48$, $\alpha = 0.04$ MPa
$\gamma_0^{\mathrm{f}} = 0.005$ MPa/s, $\gamma_{\mathrm{sat}}^{\mathrm{f}} = 0.00035$ MPa/s, $\rho = 30$, $\beta = 40.0$

where α and β are positive material parameters controlling the nonlinearity. $\bar{\tau}^{\mathrm{f}} = \sqrt{\frac{3}{2}}\|\boldsymbol{\tau}^{\mathrm{f}}\|$ is the effective value of $\boldsymbol{\tau}^{\mathrm{f}}$. Considering a 1D problem, Eq. (24b) can be integrated as

$$\tau^{\mathrm{f}} = \alpha\left(\exp\left(\beta h^{\mathrm{e}}\right) - 1\right), \quad (26)$$

where τ^{f} and h^{e} are the axial Kirchhoff stress (related to the fiber assembly) and elastic Hencky strain, respectively.

The logarithmic form of Eq. (10) is further given as

$$\overset{\circ}{\boldsymbol{\tau}}{}^{\mathrm{log}} = \overset{\circ}{\boldsymbol{\tau}}{}^{\mathrm{log(b)}} + \overset{\circ}{\boldsymbol{\tau}}{}^{\mathrm{log(f)}}, \quad (27)$$

Considering the co-directionality, corresponding to the classical notion of maximal dissipation, $\mathbf{D}^{\mathrm{vp(b)}}$ and $\mathbf{D}^{\mathrm{vp(f)}}$ are evolved as

$$\mathbf{D}^{\mathrm{vp(b)}} = \gamma^{\mathrm{b}}\boldsymbol{\tau}'^{\mathrm{b}}, \quad \mathbf{D}^{\mathrm{vp(f)}} = \gamma^{\mathrm{f}}\boldsymbol{\tau}'^{\mathrm{f}}, \quad (28)$$

where γ^{b} and γ^{f} are nonnegative coefficients controlling the evolution of ratcheting of material. It is readily obtained

that the dissipative inequality given in Eq. (22) holds. Based on the experimental observations by Gao et al. (2015), the ratcheting strain rate of articular cartilage decreases with the loading cycle number. In addition, it was further found that the ratcheting strain evolution was mainly controlled by γ^{f}. Therefore, γ^{f} is assumed to be evolved as

$$\gamma^{\mathrm{f}} = \gamma_0^{\mathrm{f}} + \left(\gamma_{\mathrm{sat}}^{\mathrm{f}} - \gamma_0^{\mathrm{f}}\right)\left(1 - \exp\left(-\rho p^{\mathrm{f}}\right)\right), \tag{29}$$

where ρ is the positive material parameter controlling the evolution of γ^{f}; γ_0^{f} and $\gamma_{\mathrm{sat}}^{\mathrm{f}}$ are respectively the initial and saturated value of γ^{f}; p^{f} is the accumulated plastic strain related to $\mathbf{D}^{\mathrm{vp(f)}}$, the rate of which is defined as

$$\dot{p}^{\mathrm{f}} = \sqrt{\frac{2}{3}}\left\|\mathbf{D}^{\mathrm{vp(f)}}\right\|. \tag{30}$$

The proposed model is summarized in Table 1.

3 Results

In this section, the prediction ability of the proposed model to describe the ratcheting behavior of articular cartilage is validated by comparing the simulations with the related experimental data by Gao et al. (2015). Note that all the calculations are done by MATLAB, and an explicit integration algorithm is adopted in the numerical implementation of the proposed model for simplification. A brief description of the explicit stress integration algorithm is given in Appendix 2.

Three loading cases were investigated: (1) a compression-unloading test with a stress variation of 0.5 MPa and a stress rate of 0.1 MPa/s to study the stress-strain hysteresis loops and the ratcheting strain evolution; (2) compression-unloading test with varied stress variations and a stress rate of 0.1 MPa/s (load case A as listed in Table 2); (3) compression-unloading test with a stress variation of 0.5 MPa and varied stress rates (load case B as listed in Table 2).

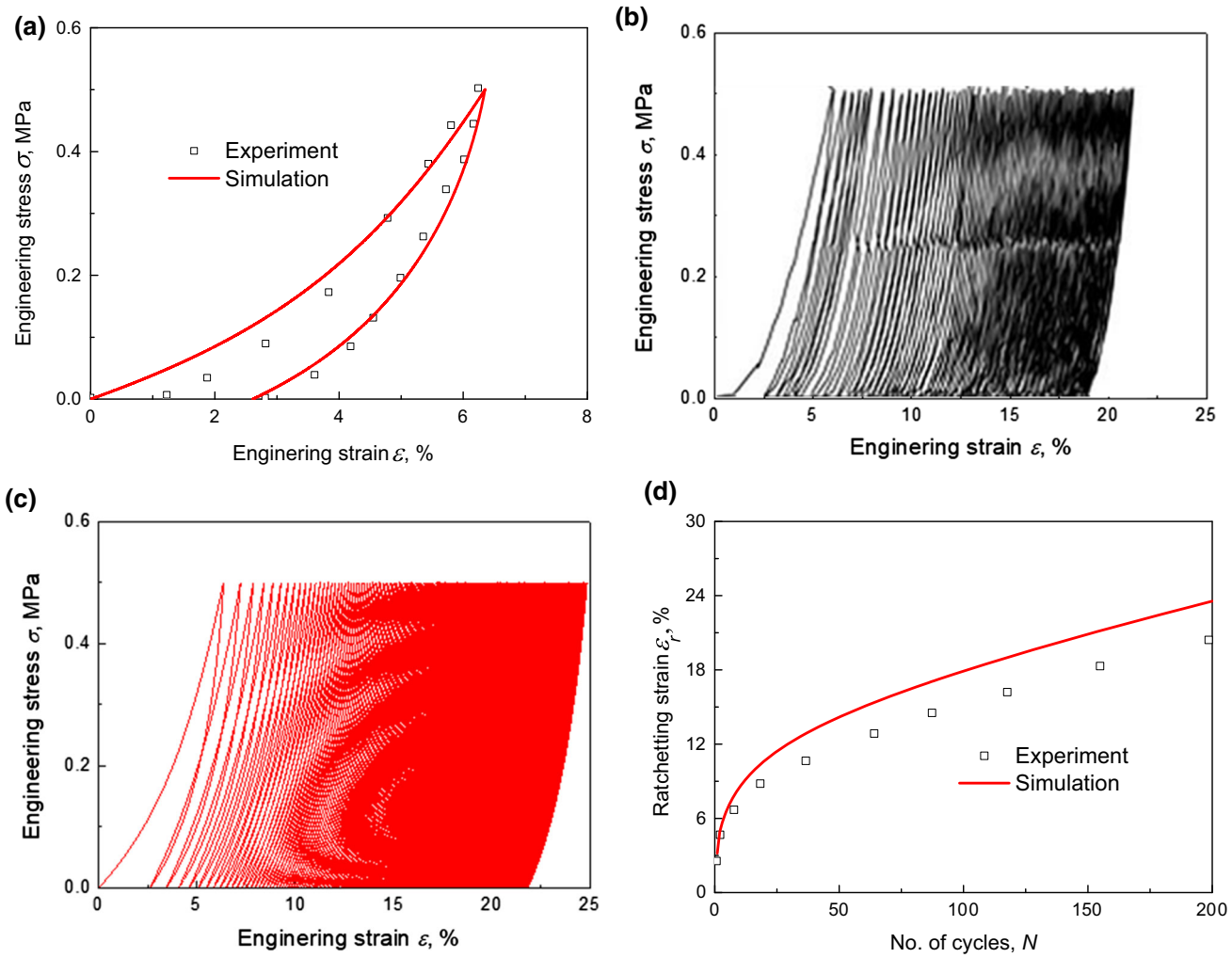

Fig. 2 Experimental and simulated biomechanical behavior of articular cartilage under compression-unloading conditions

It should be noted that the applied stress and measured strain in the experiments are the engineering ones. To be consistent, the simulated Kirchhoff stress and Hencky strain are therefore converted into engineering stress and strain with the following equations:

$$\varepsilon = \exp(h) - 1, \tag{31}$$

and

$$\sigma = \frac{\tau}{1+\varepsilon}, \tag{32}$$

where ε and h are the axial engineering and Hencky strains, respectively; σ and τ are *axial engineering and Kirchhoff stresses*, respectively.

According to Gao et al. (2013, 2015), the ratcheting strain ε_r is defined as

$$\varepsilon_r = \frac{1}{2}(\varepsilon_{\max} + \varepsilon_{\min}), \tag{33}$$

where $\varepsilon_{\max}$ and $\varepsilon_{\min}$ are respectively the maximum and minimum axial strain in a loading cycle.

All the material parameters are determined by the method in Appendix 1 and listed in Table 3. In Table 3, γ^{b} is determined from the stress-strain curve in the first cycle of the compression-unloading test with a stress variation of 0.5 MPa and a stress rate of 0.1 MPa/s; γ_0^{f}, $\gamma_{\mathrm{sat}}^{\mathrm{f}}$ and ρ are determined from the ratcheting data of the same loading case.

Figure 2 gives the simulated and related experimental stress-strain response and ratcheting behavior of articular cartilage under compression-unloading conditions. It is seen that the proposed model can reasonably simulate the stress-strain hysteresis loops (Fig. 2a–c) and the two-stage (i.e., the ratcheting strain rate decreases rapidly in the initial stage and tends to a nearly constant value after certain cycles) ratcheting behavior (Fig. 2d). However, such good simulations are expected because the material parameters listed in Table 3 are obtained from fitting of the corresponding experimental data.

The simulated and the related experimental ratcheting strain evolutions for the prescribed load cases A and case B are illustrated in Fig. 3. The figure implies that the proposed model can also capture the effect of the load level and rate on the ratcheting behavior of articular cartilage. Note that the ratcheting strains for load case A with a stress amplitude of 1.0 MPa and (Fig. 3a) load case B with a stress rate of 0.1 MPa/s (Fig. 3b) are under-predicted by the proposed model. This is because the ratcheting behavior of articular cartilage may depend not only on the accumulated plastic strain but also on the loading level and loading rate. However, there are not enough experimental data (only three tests for each load case) to achieve a more reasonable ratcheting strain evolution equation. In the present work, the ratcheting strain is assumed only to depend on the accumulated plastic strain for simplification (as shown in Eq. 29). Hence, there are deviations between the experimental and simulated ratcheting strains for some loading cases when adopting such a simple ratcheting strain evolution equation. In a future work, a modified ratcheting strain evolution equation will be proposed based on systematic experimental research on the effect of the loading level and rate on the ratcheting behavior of articular cartilage.

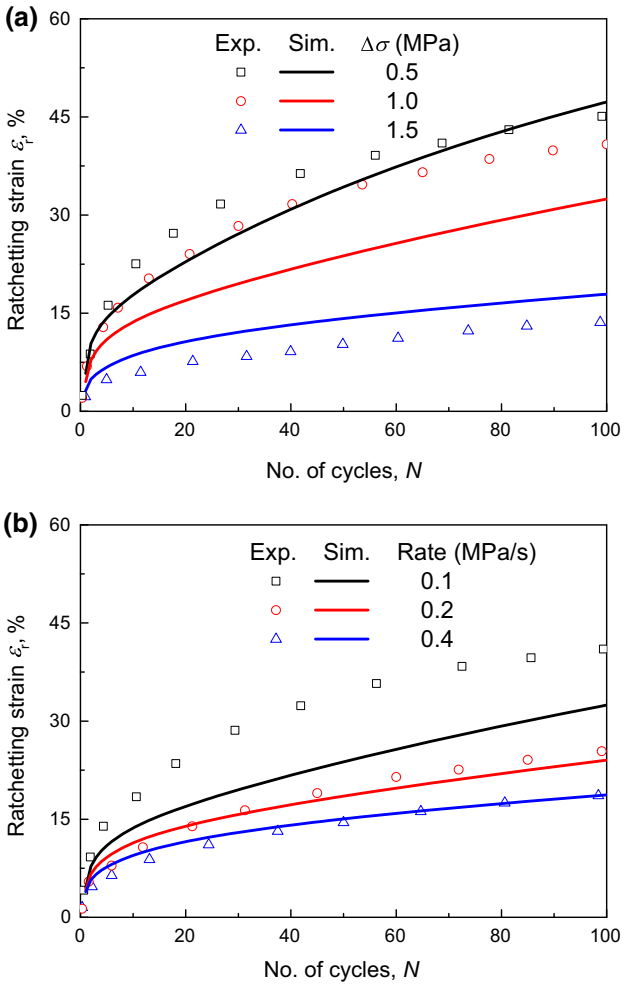

Fig. 3 Experimental and simulated ratcheting behavior of articular cartilage in **a** load case A and **b** load case B

4 Conclusions

This article seeks to propose a constitutive model to describe the ratcheting behavior of articular cartilage in the framework of finite elasto-viscoplastic theory by adopting the logarithmic stress rate. The constitutive equations are formulated based on the microstructure of articular cartilage. The predictive ability of the proposed model is validated by

benchmarking the simulations with the related experimental data. The following conclusions can be drawn.

1. The proposed constitutive model is thermodynamically consistent.
2. Based on experimental observation, the articular cartilage is simplified as a composite that consists of a fiber assembly (related to the collagen fibers) and a soft basis (related to the other components). The free energy function and stress tensor are divided into two contributions accordingly.
3. The proposed model can reasonably describe the hysteresis loops and the dependence of the loading level and loading rate on the ratcheting behavior of articular cartilage under cyclic compression-unload conditions. However, there are large deviations between the experimental and simulated ratcheting strains for some loading cases because only a simple ratcheting strain evolution equation was adopted in the present work.

Funding This study was funded by the National Natural Science Foundation of China (11702036) and Chengdu University New Faculty Start-up Funding (2081915038).

Compliance with ethical standards

Conflict of interest The authors declare that they have no conflict of interest.

Appendix 1: Material parameter determination

The elastic and viscoplastic parameters are coupled with each other. To simplify the material parameter determination process, a two-step method is adopted as follows:

Step 1: Determine the elastic parameters, i.e., E^{b}, ν^{b}, α, β and ν^{f}, roughly by neglecting the viscoplastic deformation, and then obtain the viscoplastic parameters based on the coarse elastic materials.

Neglecting viscoplastic deformation, it can be obtained from Eqs. (10), (24) and (26)

$$\tau \approx E^{\mathrm{b}} h + \alpha(\exp(\beta h) - 1). \tag{34}$$

The strength of articular cartilage in the initial stage is mainly supported by the basis, and the stress-strain curve is approximately linear with a quasi-linear modulus (denoted as E^{initial}), which is much smaller than that after a moderate deformation (referring to Gao et al. 2015). It is indicated that E^{b} contributes a very small proportion of the total modulus. Therefore, E^{b} can be set as E^{initial} for simplification. Once E^{b} has been determined, α and β can be easily determined from a tension/compression stress-strain curve $\tau \sim h$.

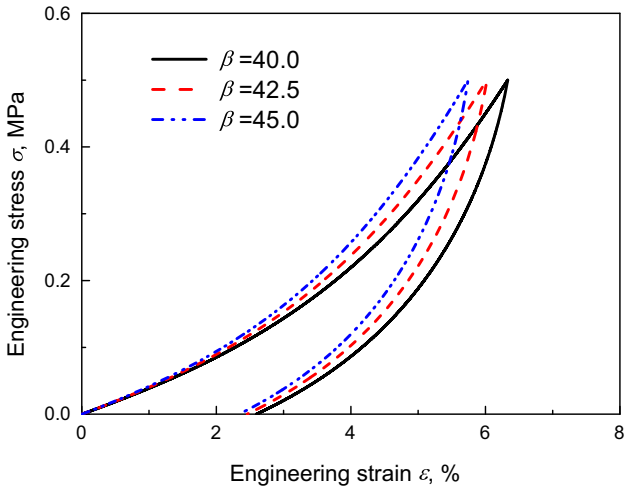

Fig. 4 Simulated stress-strain hysteresis loop of the first cycle with varied β (the other parameters are identical to those listed in Table 3) for the compression-unloading test with a stress variation of 0.5 MPa and a stress rate of 0.1 MPa/s

Once E^{b} has been determined, α and β can be easily determined from a tension/compression stress-strain curve $\tau \sim h$.

Since the fluid phase accounts for about 80% of articular cartilage (Mow et al. 1980), the material can be considered as approximately incompressible. Therefore, ν^{b} and ν^{f} can be close to 1/2.

It was also found that the stress-strain hysteresis loops are mainly dependent on E^{b} and γ^{b}. In addition, the choice of E^{b} and ν^{b} hardly affects the simulated ratcheting strain since the proportion of $\boldsymbol{\tau}^{\mathrm{b}}$ is very small. Therefore, once E^{b} has been given, γ^{b} is determined from a stress-strain curve in the loading-unloading condition by a trial-and-error method.

The ratcheting is mainly controlled by γ_0^{f}, $\gamma_{\mathrm{sat}}^{\mathrm{f}}$ and ρ. These parameters are determined from a ratcheting test by a trial-and-error method.

Step 2: Refine the elastic parameters based on the determined viscoplastic parameters.

Since the plastic deformation is neglected when determining the elastic parameters, the material parameters obtained in Step 1 are relatively coarse and hence need to be refined to predict the material responses more reasonably. Figures 4 and 5 illustrate the hysteresis loop of the first cycle and ratcheting strain (in the compression-unloading test with a stress variation of 0.5 MPa and a stress rate of 0.1 MPa/s) predicted by the proposed model with varied β and the other parameters listed in Table 3. It is indicated that: (1) the predicted stress-strain response can be fitted by adjusting the parameter β (Fig. 4); (2) modifying the elastic parameter β has almost no influence on the predictions of the stress-strain hysteresis and the ratcheting behavior (Figs. 4, 5). In other words, only the elastic parameter β needs to be refined in this step.

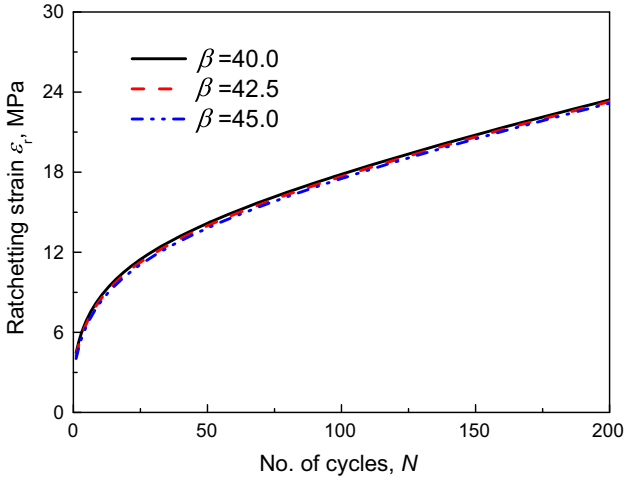

Fig. 5 Simulated ratcheting strain evolution with varied β (the other parameters are identical to those listed in Table 3) for the compression-unloading test with a stress variation of 0.5 MPa and a stress rate of 0.1 MPa/s

Appendix 2: Explicit numerical integration procedure

In this appendix, the explicit numerical integration procedure is briefly given. Assuming that an initial natural state of the considered body corresponds to the moment $t=0$, i.e.,

$$\boldsymbol{\tau}|_{t=0},\ \mathbf{F}|_{t=0} = \mathbf{R}^{\log}|_{t=0} = \mathbf{1}. \tag{35}$$

Then, considering the interval from steps n to $n+1$ with a time increment $\Delta t = t_{n+1} - t_n$, it is assumed that the components $\boldsymbol{\tau}_n, \boldsymbol{\tau}_n^{\mathrm{b}}, \boldsymbol{\tau}_n^{\mathrm{f}}, p_n^{\mathrm{f}}, \mathbf{F}_n, \mathbf{L}_n, \mathbf{D}_n, \mathbf{W}_n, \boldsymbol{\Omega}_n^{\log}$ and $\mathbf{R}_n^{\log}$ in the step n are all known. The increment of the deformation gradient $\Delta\mathbf{F}_{n+1}$ in step $n+1$ is given.

Step 1: Calculating the stretching spin tensors and Hencky strain

$$\mathbf{F}_{n+1} = \mathbf{F}_n + \Delta\mathbf{F}_{n+1}. \tag{36}$$

$$\mathbf{L}_{n+1} = \frac{(\mathbf{F}_{n+1} - \mathbf{F}_n)}{\Delta t}\mathbf{F}_{n+1}^{-1}. \tag{37}$$

$$\mathbf{D}_{n+1} = \mathrm{sym}\mathbf{L}_{n+1}, \quad \mathbf{W}_{n+1} = \mathrm{skw}\mathbf{L}_{n+1}. \tag{38}$$

$$\mathbf{h}_{n+1}^{\mathrm{b}} = \mathbf{h}_{n+1}^{\mathrm{f}} = \mathbf{h}_{n+1} = \ln\mathbf{V}_{n+1} = \ln\sqrt{\mathbf{F}_{n+1}\mathbf{F}_{n+1}^{\mathrm{T}}}. \tag{39}$$

Step 2: Calculating the logarithmic spin and rotation

Details of the the calculation of the logarithmic spin $\boldsymbol{\Omega}_{n+1}^{\log}$ can be found in Zhu et al. (2014a). Once $\boldsymbol{\Omega}_{n+1}^{\log}$ has been obtained, the logarithmic rotation $\mathbf{R}_{n+1}^{\log}$ can be calculated as

$$\mathbf{R}_{n+1}^{\log} = \exp\left(\boldsymbol{\Omega}_{n+1}^{\log}\Delta t\right)\mathbf{R}_n^{\log}. \tag{40}$$

Step 3: Calculating the viscoplastic stretching tensors, accumulated plastic strain and ratcheting coefficient.

$$\mathbf{D}_{n+1}^{\mathrm{vp(b)}} = \gamma_n^{\mathrm{b}}\boldsymbol{\varnothing}'^{\mathrm{b}}_n, \quad \mathbf{D}_{n+1}^{\mathrm{vp(f)}} = \gamma_n^{\mathrm{f}}\boldsymbol{\varnothing}'^{\mathrm{f}}_n. \tag{41}$$

$$p_{n+1}^{\mathrm{f}} = p_n^{\mathrm{f}} + \sqrt{\frac{2}{3}}\left\|\mathbf{D}_{n+1}^{\mathrm{vp(f)}}\right\|. \tag{42}$$

$$\gamma^{\mathrm{f}} = \gamma_0^{\mathrm{f}} + \left(\gamma_{\mathrm{sat}}^{\mathrm{f}} - \gamma_0^{\mathrm{f}}\right)\left(1 - \exp\left(-\rho p_{n+1}^{\mathrm{f}}\right)\right). \tag{43}$$

Step 4: Calculating the stress tensors

$$\mathbf{D}_{n+1}^{\mathrm{e(b)}} = \mathbf{D}_{n+1}^{\mathrm{b}} - \mathbf{D}_{n+1}^{\mathrm{vp(b)}}, \quad \mathbf{D}_{n+1}^{\mathrm{e(f)}} = \mathbf{D}_{n+1}^{\mathrm{f}} - \mathbf{D}_{n+1}^{\mathrm{vp(f)}}. \tag{44}$$

$$E^{\mathrm{f}} = \beta\left(\alpha + \bar{\tau}_{n+1}^{\mathrm{f}}\right). \tag{45}$$

$$\boldsymbol{\tau}_{n+1}^{\mathrm{b}} = \mathbb{C}^{\mathrm{b}} : \mathbf{D}_{n+1}^{\mathrm{e(b)}}\Delta t + \Delta\mathbf{R}_{n+1}\boldsymbol{\tau}_n^{\mathrm{b}}\Delta\mathbf{R}_{n+1}^{\mathrm{T}}. \tag{46}$$

$$\boldsymbol{\tau}_{n+1}^{\mathrm{f}} = \mathbb{C}^{\mathrm{f}} : \mathbf{D}_{n+1}^{\mathrm{e(f)}}\Delta t + \Delta\mathbf{R}_{n+1}\boldsymbol{\tau}_n^{\mathrm{f}}\Delta\mathbf{R}_{n+1}^{\mathrm{T}}. \tag{47}$$

$$\boldsymbol{\tau}_{n+1} = \boldsymbol{\tau}_{n+1}^{\mathrm{b}} + \boldsymbol{\tau}_{n+1}^{\mathrm{f}}. \tag{48}$$

In Eqs. (46) and (47), $\Delta\mathbf{R}_{n+1}$ is denoted as

$$\Delta\mathbf{R}_{n+1} = \left(\mathbf{R}_n^{\log}\right)^T\mathbf{R}_{n+1}^{\log}. \tag{49}$$

References

Ahmadzadeh G, Varvanifarahani A (2015) Ratcheting prediction of Al 6061/SiCP composite samples under asymmetric stress cycles by means of the Ahmadzadeh-Varvani hardening rule. J Compos Mater 50(17):2389–2397

Armstrong CG, Lai WM, Mow VC (1984) An analysis of the unconfined compression of articular cartilage. J Biomech Eng 106:165–173

Ateshian GA (2017) Mixture theory for modeling biological tissues: illustrations from articular cartilage. Springer, London

Athanasiou K, Darling E, Hu J (2009) Articular cartilage tissue engineering. Synth Lect Tissue Eng 1(1):1–182

Barker MK, Seedhom BB (2001) The relationship of the compressive modulus of articular cartilage with its deformation response to cyclic loading: does cartilage optimize its modulus so as to minimize the strains arising in it due to the prevalent loading regime? Rheumatology 40:274–284

Bellucci G, Seedhom BB (2001) Mechanical behaviour of articular cartilage under tensile cyclic load. Rheumatology 40:1337–1345

Bruhns OT, Xiao H, Meyers A (1999) Self-consistent Eulerian rate type elasto-plasticity models based upon the logarithmic stress rate. Int J Plast 15:479–520

Bursać PM, Obitz TW, Eisenberg SR, Stamenović D (1999) Confined and unconfined stress relaxation of cartilage: appropriateness of a transversely isotropic analysis. J Biomech 32:1125–1130

Chen X, Hui S (2005) Ratcheting behavior of PTFE under cyclic compression. Polym Test 24:829–833

Gao LL, Zhang CQ, Yang YB, Shi JP, Jia YW (2013) Depth-dependent strain fields of articular cartilage under rolling load by the optimized digital image correlation technique. Mater Sci Eng, C 33:2317–2322

Gao LL, Qin XY, Zhang CQ, Gao H, Ge HY, Zhang XZ (2015) Ratcheting behavior of articular cartilage under cyclic unconfined compression. Mater Sci Eng C Mater Biol Appl 57:371–377

García JJ, Cortés DH (2006) A nonlinear biphasic viscohyperelastic model for articular cartilage. J Biomech 39:2991

Guo S, Kang G, Zhang J (2013) A cyclic visco-plastic constitutive model for time-dependent ratchetting of particle-reinforced metal matrix composites. Int J Plast 40:101–125

Huang CY, Mow VC, Ateshian GA (2001) The role of flow-independent viscoelasticity in the biphasic tensile and compressive responses of articular cartilage. J Biomech Eng 123:410–417

Kang G (2008) Ratchetting: recent progresses in phenomenon observation, constitutive modeling and application. Int J Fatigue 30:1448–1472

Kang G, Wu X (2011) Ratchetting of porcine skin under uniaxial cyclic loading. J Mech Behav Biomed Mater 4:498–506

Kerin AJ, Coleman A, Wisnom MR, Adams MA (2003) Propagation of surface fissures in articular cartilage in response to cyclic loading in vitro. Clin Biomech 18:960

Kurz B, Lemke AK, Fay J, Pufe T, Grodzinsky AJ, Schünke M (2005) Pathomechanisms of cartilage destruction by mechanical injury. Ann Anat 187:473–485

Kwan MK, Lai WM, Mow VC (1990) A finite deformation theory for cartilage and other soft hydrated connective tissues–I. Equilibrium results. J Biomech 23:145–155

Li LP, Herzog W, Korhonen RK, Jurvelin JS (2005) The role of viscoelasticity of collagen fibers in articular cartilage: axial tension versus compression. Med Eng Phys 27:51–57

Lu F, Kang G, Zhu Y, Xi C, Jiang H (2016) Experimental observation on multiaxial ratchetting of polycarbonate polymer at room temperature. Polym Test 50:135–144

Matzat SJ, Van TJ, Gold GE, Oei EH (2013) Quantitative MRI techniques of cartilage composition. Quant Imaging Med Surg 3:162–174

Mow VC, Kuei SC, Lai WM, Armstrong CG (1980) Biphasic creep and stress relaxation of articular cartilage in compression: theory and experiments. J Biomech Eng 102:73

Pierce DM, Ricken T, Holzapfel GA (2013) A hyperelastic biphasic fibre-reinforced model of articular cartilage considering distributed collagen fibre orientations: continuum basis, computational aspects and applications. Comput Methods Biomech Biomed Eng 16:1344–1361

Responte DJ, Natoli RM, Athanasiou KA (2007) Collagens of articular cartilage: structure, function, and importance in tissue engineering. Crit Rev Biomed Eng 35:363–411

Seifzadeh A, Oguamanam DC, Trutiak N, Hurtig M, Papini M (2012) Determination of nonlinear fibre-reinforced biphasic poroviscoelastic constitutive parameters of articular cartilage using stress relaxation indentation testing and an optimizing finite element analysis. Comput Methods Programs Biomed 107:315–326

Soltz MA, Ateshian GA (2000a) A conewise linear elasticity mixture model for the analysis of tension-compression nonlinearity in articular cartilage. J Biomech Eng 122:576

Soltz MA, Ateshian GA (2000b) Interstitial fluid pressurization during confined compression cyclical loading of articular cartilage. Ann Biomed Eng 28:150–159

Sophia Fox AJ, Bedi A, Rodeo SA (2009) The basic science of articular cartilage: structure, composition, and function Sports. Health 1:461–468

Wilson W, van Donkelaar CC, Van RB, Huiskes R (2005) A fibril-reinforced poroviscoelastic swelling model for articular cartilage. R.G. Landes Co

Xiao H, Bruhns DIOT, Meyers DIA (1997a) Logarithmic strain, logarithmic spin and logarithmic rate. Acta Mech 124:89–105

Xiao H, Bruhns OT, Meyers A (1997b) Hypo-elasticity model based upon the logarithmic stress rate. J Elast 47:51–68

Zhu Y, Kang G, Kan Q, Bruhns OT (2014a) Logarithmic stress rate based constitutive model for cyclic loading in finite plasticity. Int J Plast 54:34–55

Zhu Y, Kang G, Kan Q, Yu C (2014b) A finite viscoelastic-plastic model for describing the uniaxial ratchetting of soft biological tissues. J Biomech 47:996

Zhu Y, Kang G, Kan Q, Bruhns OT, Liu Y (2016) Thermo-mechanically coupled cyclic elasto-viscoplastic constitutive model of metals: theory and application. Int J Plast 79:111–152